Proceedings of ERAD 2006

Fine tuning of Radar Rainfall Estimates based on Bias and Standard Deviations Adjustments

Angel Luque, Alberto Martín, Romualdo Romero, Sergio Alonso

University of Balearic Island, Palma de Mallorca (Spain)

1 Introduction

This paper assesses the accuracy with which single radar 1.5 km CAPPI imagery and 2 by 2 km resolution can be used to estimate precipitation in the 9-10 June 2000 Montserrat flash flood episode in Catalonia, Spain (Llasat et al., 2002). Results using $Z=A\cdot R^B$ (Marshal and Palmer Z-R relationship, 1948) with coefficients for stratiform (A=200, B=1.6) and convective (A=800, B=1.6) rain are compared with those obtained using the Histogram Matching Technique (HMT) as perform by Crosson et al. (1996) and compared, also, with a Direct Calibration Method (DCM). 5 min. rainfall series of 126 automatic raingauges of the Agency Catalana of Water (ACA), well distributed over the damaged area by the flood, were used during the calibration process and to generate rain accumulations for the verification phase. Radar precipitation amounts are clearly underestimated for this flood case when using standard Marshal and Palmer Z-R relationships and coefficients. Short time calibration performed using the HMT or by the DCM can solve this problem. In addition, post-calibration fine tuning alternatives were explored for both, HMT and DCM, based on bias and standard deviations adjustments by keeping correlations and squared errors almost unchanged.

2 Methodology

Radar reflectivies are associated with interpolated rain rates using a kriging analysis method from the ACA network collocated in time and space during the hours of heaviest rainfalls. Radar-rain points were recorded in a period of 5 hours every 30 minutes to generate the calibration dataset. The data collecting process covered from 00:20 to 05:20 UTC on 10 June. This dataset pretend to capture the main rainfall patterns of the Montserrat storm. It was used to delineate Z-R relationships by the HMT and the DCM. The verification was performed from 21:00 to 09:00 divided in four periods of three hours of rainfall accumulations for qualitative and numerical comparison. The statistical indices employed in the quantitative verification in the area well covered by the rain gauges are: mean, standard deviation (SD), BIAS, standard deviations difference (SDD), root mean square error (RMS), and correlation coefficient (CORR). For rain rates have been computed other parameters to test the spatial accuracy of points greater than zero mm·h^{-1}. Those are: Probability of detection (POD), false alarm ratio (FAR), critical success index (CSI) and fraction correct (FRC) (Marzban, 1998).

3 Histogram Matching Technique (HMT)

The principle of the HMT is to construct a Z-R relationship based on (Zi, Ri) pairs such that cumulative distribution functions (CDFs) of Z and R match; that is, Pairs that satisfy.

$$\int_{Rt}^{Ri} P(R)\cdot dR = \int_{Zt}^{Zi} P(Z)\cdot dZ \qquad (1)$$

where $P(R)$ represents a probability density function and Rt and Zt are threshold values. In this paper we are following the modified procedure described by Atlas et al. (1990), in which the CDFs are derived for the first moments of Z and R according to:

$$\frac{\int_{Rt}^{Ri} R\cdot P(R)\cdot dR}{\int_{Rt}^{\infty} R\cdot P(R)\cdot dR} = \frac{\int_{Zt}^{Zi} Z\cdot P(Z)\cdot dZ}{\int_{Zt}^{\infty} Z\cdot P(Z)\cdot dZ} \qquad (2)$$

In practice, the (Zi, Ri) values are found by approximating (2) with discrete summations. To determine the CDFs of Z and R and calculate the Z-R relationship from (2), the threshold values Rt and Zt must be defined. In the case of Rt, the minimum detectable rain rate in 0.2 mm·h^{-1}. Zt is then

Correspondence to: Angel Luque.

Angel.luque@uib.es

chosen so that the percent of the space-time domain over which $Z \geq Zt$ is equivalent to the percent of the space-time domain for which $R \geq Rt$. All the points from the calibration dataset with a rainfall greater than 0.2 mm·h^{-1} is equalized with the number of radar points with a logarithmic reflectivity of 7.5 dBZ or greater. In summary, Rt = 0.2 mm·h^{-1} and Zt = 7.5 dBZ in our calculations.

Based on the threshold values Rt and Zt the conditional CDFs of R and Z were calculated at 3-mm·h^{-1} and 3 dBZ intervals and plotted in Fig 1 as the HMT curve.

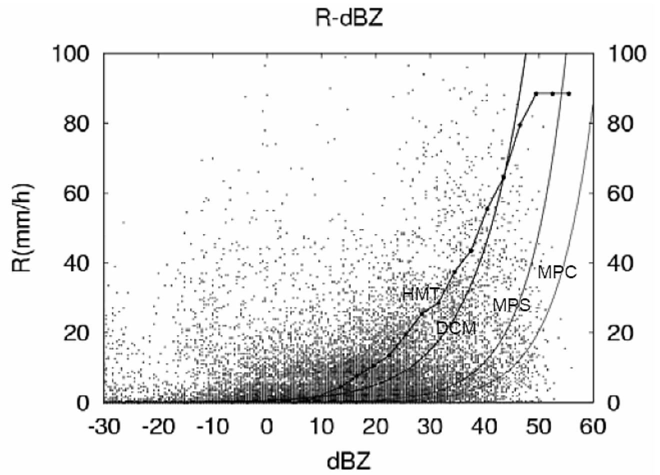

Fig. 1. Measured radar-rain points from the calibration file, HMT DCM, MPS and MPC rainfall curves.

The calibration dataset is used also to validate the HMT method for this case by transforming Z from the radar to R using the HMT curve and computing the statistics shown in the inset table on Fig 2. An analysis of these numerical results demonstrates that relative errors in the BIAS are greater than 40 % and larger than 45 % in the SSD. Those errors were minimized by shifting the entire HMT curve in the logarithmic scale to the right as shown in Fig 2a. Statistics were computed iteratively after each Z increment of one dBZ (dBZ'= +1.0) and plotted in Fig 2b. After few iterations (dBZ'= + 4.0) the BIAS was closer to 0 while error in SSD was reduced to 20 %. Reflectivities were corrected by just moving the curve 4 dBZ. Only the threshold values, Rt and Zt, stay the same as shown in this table and in Fig 2, in order to not change the size of the radar-gauge rain areas and to not decrease the accuracy of the rain detection (POD, FAR, CSI and FRC do not change in Fig 2 after the bias adjustment).

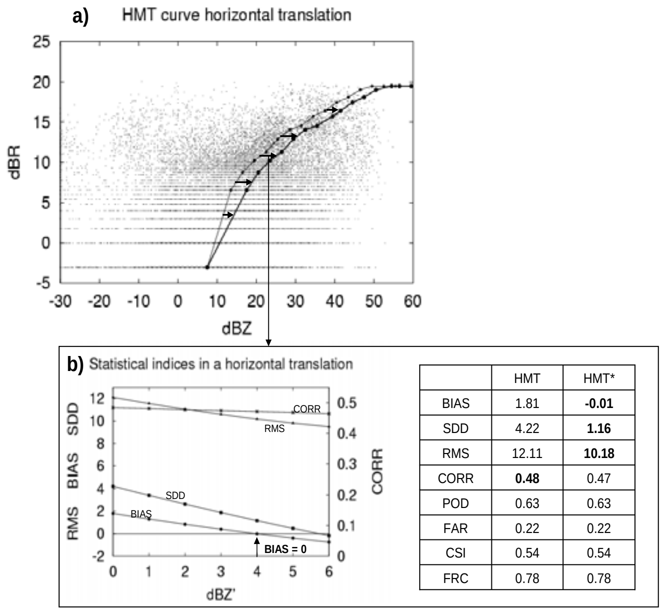

	HMT	HMT*
BIAS	1.81	**-0.01**
SDD	4.22	**1.16**
RMS	12.11	**10.18**
CORR	**0.48**	0.47
POD	0.63	0.63
FAR	0.22	0.22
CSI	0.54	0.54
FRC	0.78	0.78

Fig. 2. **(a)** Radar-rain points from the calibration file and HMT curve in the logarithmic scale (*dBR=10·log(R)*). **(b)** evolution of statistical indices with respect to dBZ'. When the BIAS is closer to cero the translation is ended and statistical results are written in the contiguous table. The table show the Statistics before (HMT) and after the BIAS adjustment (HMT*).

4 Direct Calibration Method (DCM)

The DCM is based on the $Z=A\cdot R^B$ relationship derived from the drop size distribution (Marshall and Palmer, 1948). This relation is linear in the logarithmic scale where Z and R are transformed as $dBR=10\cdot log(R)$ and $dBZ=10\cdot log(Z)$, so:

$$dBZ = 10\cdot log(A) + B\cdot dBR \qquad (3)$$

The coefficients A and B are easily determined from the linear best fit using the Z-R point data from the calibration file. The best-fit equation was found to be

$$dBZ = -50.8131 + 9.4200\cdot dBR \qquad (4)$$

in which A=8.2925·10^{-6} and B=9.4200. dBR was inversely transformed to R and left as a function of dBZ as shown in the next equation.

$$R(dBZ) = 10^{\left[\frac{dBZ - 10\cdot\log(A)}{10\cdot B}\right]} \qquad (5)$$

A preliminary evaluation of these new A and B coefficients confirm that estimated rainfall leads to a bias due to the dominance of the zero and light rain observations. This effect has been corrected empirically case after two steps:

- A Rotation of the calibration regression line in order to increment the slope (Figs 3a and 3b). This process, applied one by one degree, increases the importance of higher rain rates and increases the dispersion of the estimated rainfall measured by the SDD. The centre of rotation was selected searching the point on the line surrounded by as many radar-rain points as possible. Statistical indices and centre of rotation were calculated iteratively after each increment of the line slope as shown in Fig 3b. The process continued until the SDD was closest to zero yielding an angle of 25º.

- Horizontal translation of the rotated calibration line (Figs 3a and 3c). One way to adjust the BIAS while keeping the CORR unchanged is moving the line in the horizontal direction without changing the slope. A translation of 3 dBZ to the left (dBZ'= -3) led to a BIAS close to zero and to an increment of 30% of the SDD (Fig 3c). This increment can be considered reasonable because radar rain distributions are more spread and irregular than the interpolated rain field from the rain gauges.

Finally, the resulting calibration line equation and A, B coefficients after the two processes are:

$$dBZ = 4.8268 + 2.1386 \cdot dBR \qquad (6)$$

A=3.0386, B=2.13869. Spatial accuracy of radar rainfall is, also, improved as shown by the CSI and FRC indices in Fig 3. DCM curve using those coefficients is shown in Fig 1.

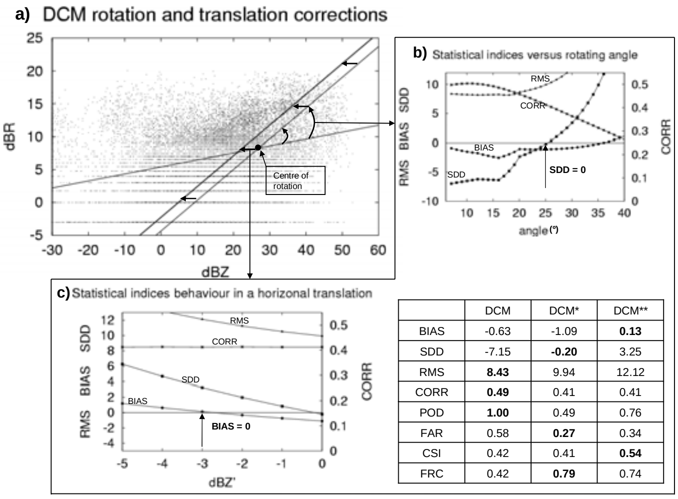

	DCM	DCM*	DCM**
BIAS	-0.63	-1.09	**0.13**
SDD	-7.15	**-0.20**	3.25
RMS	**8.43**	9.94	12.12
CORR	**0.49**	0.41	0.41
POD	**1.00**	0.49	0.76
FAR	0.58	**0.27**	0.34
CSI	0.42	0.41	**0.54**
FRC	0.42	**0.79**	0.74

Fig. 3. (a) DCM calibration straight line from equation 4 firstly rotated and secondly translated in the logarithmic scale. (b) Behavior of statistical indices with respect to the angle of rotation. Statistical results are shown in the second column of the table (DCM*) for the angle in which the SDD is closer to 0. (c) Evolution of statistical indices for the DCM line shifting. This process is done until the BIAS is closer to 0 and at this point results are written in the last column of the table (DCM**).

5 Standards methods (MPS, MPC).

Are based on the use of the Marshal and Palmer Z-R relationship taking into account coefficients for stratiform rain (A=200, B=1.6) and convective rain (A=800, B=1.6) according to the bibliography (Marshal and Palmer, 1942). In practice rain fields were computed transforming *dBZ* to *R* using equation 5 but changing the A and B coefficients in each case. In the present research, radar rain fields obtained by the Marshal and Palmer stratiform rain coefficients are called MPS and the ones obtained with the convective coefficients are called MPC and are shown in Fig 1.

6 Results

The observed accumulated rainfall from the ACA network during 3 hours time spans for the period of heaviest precipitation of the Montserrat event is illustrated in Fig 4 and the corresponding radars ones, in Fig 5. Most of the rainfalls occurred from 21:00 UTC 9 June to 06:00 UTC the next day but only the period between 00:00 to 03:00 is shown in the figures. The spatial distributions are very similar among the different calibration methods (HMT, DCM, MPS and MPC). It is notable the ability of radar capturing fine details of the precipitation fields. The HMT and DCM accumulations are very close to the ones measured by the ACA network. The MPS and MPC accumulations are in general, 20 mm and 40 mm below the observed amounts respectively.

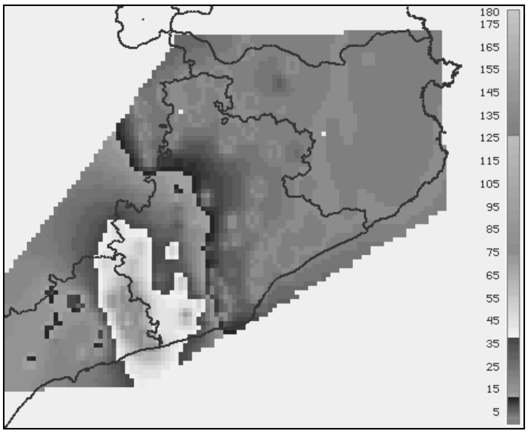

Fig. 4. Observed 3 hours accumulated rainfall from 00:00 to 03:00 10 June 2000. Accumulations from the ACA rain gauges are spatially interpolated by the kriging analysis method and used as ground true for the verification of the radar accumulations. Only the area best covered by rain gauges is considered.

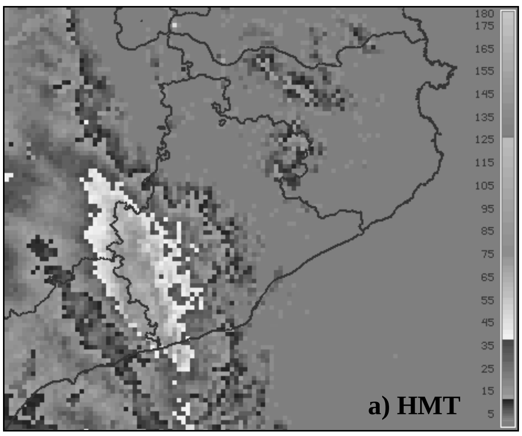

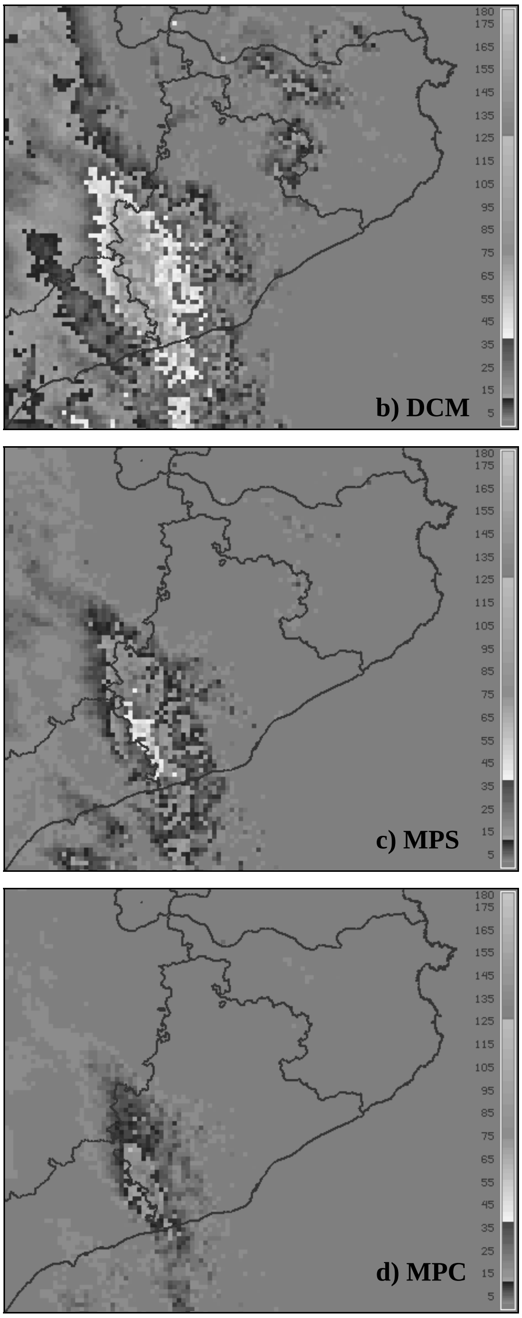

Fig. 5. 3 hours radar accumulated rainfall performed by the different algorithms for the same period than Fig 4.

A numerical analysis is important to determine the accuracy of the radar precipitation estimated by the different methods and to determine the best one. Statistical indices in table 1 show that the HMT provides the best spatial skill with a CORR of 0.78 and the best precipitation amounts with a BIAS around 0.99 mm (~10% relative error) and a SDD of 4.47 mm (~35% relative error). Then the DCM has a CORR of 0.76 and slightly higher BIAS and SDD. It, also, obtain the greatest RMS with 12.12 mm. The MPS and MPC methods obtain both the lowest CORRs, they have a clear tendency to under estimate accumulated precipitation as indicated by a strong negative BIAS and SDD, although the MPS gives the lowest RMS among the techniques with 9.73 mm.

Table 1. Statistical indices obtained from the gauge-radar direct comparison of accumulated rainfall in the area best covered by rain gauges (See Fig 4) and for three periods. The period between 03:00 to 06:00 was omitted because of radar attenuations problems.

	OBS	HMT	DCM	MPS	MPC	Day/period (UTC hours)
Size			16290 (5430 x 3)			
Mean	10.0	11.0	11.0	2.3	1.0	09/21-24
SD	12.6	17.0	18.4	5.3	2.3	+
BIAS		**1.0**	1.0	-7.7	-9.1	10/00-03
SDD		**4.5**	5.8	-7.3	-10.3	+
RMS		10.7	12.1	**9.7**	11.2	10/06-09
CORR		**0.78**	0.76	0.66	0.68	

7 Conclusions

The aim of this work is to demonstrate that radar and rain gauges can be combined to improve the spatial distribution of the precipitation field and to gain accurately in rainfall amounts within an operational context.

Old radar algorithms not adjusted or corrected for a specific area can produce significant errors in rainfall rates and accumulations. The HMT adjusted by the BIAS is the method with the best performance.

Our results in radar calibration are derived under the circumstances of a flood case and should not be directly applied to events in other areas and situations. Technical details are provided to develop similar methodologies in the operational context.

Acknowledgements: This research was developed under the objectives of the Interreg IIIB-Medocc European project AMPHORE (2003-03-4.3-I-079) and the Spanish project PRECIOSO MEC (CGL2005-03918/CLI). Radar data were provided by the Spanish Meteorological Institute (INM). Raingauges data of the internal basins of Catalonia were supplied by the Agencia Catalana del Agua (ACA).

References

Atlas, D., D. Rosenfeld, and D. B. Wolff, 1990: Climatologically tuned rain rate relations and links to area-time integrals, *J. Appl. Meteor.*, vol. **29**, 1120-1125.

Crosson, W.L., C.E. Duchon, R. Raghavan, and S.J. Goodman, 1996: Assessment of Rainfall Estimated Using a Standard Z-R Relationship and the Probability Matching Method Applied to composite Radar Data in Central Florida. *J. Appl. Meteor.*, **35**, 1203-1219

Llasat, M.C. et al. 2002: Diagnosis of a strong convective event produced in Catalonia on June 10, 2000. Proceedings of the 3rd EGS Plinius Conference, Sardinia, Italy, 1-3 October 2001, *GNDCI*, pub. n. **2560**, 67-70.

Marshall, J. S., and Palmer W. M. K., 1948, The distribution of raindrops with size. *J. Atmos. Sci.*, **5**, 165-166.

Marzban C., 1998, Scalar Measures of Performance in Rare-event Situations, *Wea. Forecasting*, **13**, 753-763